

CONSTRUCTION OF VISUAL THREE-DIMENSIONAL FABRIC REINFORCED COMPOSITE THERMAL PERFORMANCE PREDICTION SYSTEM

Shaofei Wu^{1,2,*}

^{*1} Hubei Province Key Laboratory of Intelligent Robots, Wuhan Institute of Technology, Wuhan, P.R.China

² School of Computer Science and Engineering, Wuhan Institute of Technology, Wuhan, P.R.China

* Corresponding author; E-mail: wasbfc@yeah.net

In view of the construction of a visualized three-dimensional thermal performance prediction system for fabric reinforced composites, the thermal constants analyzer was used to analyze and compare the thermal conductivity of the three-dimensional fabric reinforced composites by experimental methods, such as fiber volume fraction, internal braiding angle, and different yarn reduction methods and fabric structures. The factors influencing the thermal conductivity of three-dimensional fabric reinforced composites were studied, and the principle of thermal conductivity was analyzed. The thermal expansion coefficients of three-dimensional fabric reinforced composites in X and Y directions are one order of magnitude smaller than those in Z directions. When aramid fabric is used as reinforcement, the composites with negative thermal expansion coefficients can be designed. The research results provide the necessary basis for the design, application and theoretical research of the three-dimensional fabric reinforced composites in heat conduction. Through the research of this paper, it lays a foundation for the process selection, performance design and structure optimization of this kind of material, and promotes the further application of three-dimensional braided composites.

Key words: three-dimensional fabrics, composite materials, thermal properties, prediction system

1. Introduction

The properties of three-dimensional fabric reinforced composites are highly dependent on their structures due to their high heterogeneity and multi-scale internal structure. The number of layers, laying sequence and laying angle of fibers in the composite strongly affect the stress distribution of the composite under load, thus affecting its performance [1-2]. As far as three-dimensional fabric reinforced composites are concerned, accurate prediction of their performance parameters is the premise of performance-oriented design. From the point of view of current technology level, the determination of material performance parameters is mainly through referring to national/industry standards. However, the development efficiency of three-dimensional fabric reinforced composites is relatively low, the development cycle is long, and the cost is high, which makes it limited to determine the mechanical and thermal properties of three-dimensional fabric reinforced composites by experimental methods. Therefore, the rapid, accurate and effective prediction of mechanical and thermal properties of composite materials by finite element analysis has become the focus of many experts and scholars [3].

Fabric reinforced composites are the combination of composite technology and textile technology. Fabric reinforced composites are an important branch of advanced composites in the field of high technology. They have shown their unique advantages in many aspects of modern engineering technology. Fabric reinforced composites have experienced the development process from unidirectional plate to two-dimensional fabric reinforced composites, and then to three-dimensional

fabric reinforced composites [4-5]. The application of two-dimensional fabric reinforced composites in automotive industry, construction, aerospace and other fields is limited due to its manufacturing problems and some poor mechanical properties, such as low impact damage resistance, poor fracture orientation, and easy debonding between matrix and reinforcement under impact. In order to overcome the problems of fabrication and mechanical properties of two-dimensional fabric reinforced composites, domestic and foreign scholars have developed three-dimensional fabric reinforced composites by means of mechanical properties analysis, combined with the traditional manufacturing process of composite materials. Three-dimensional fabric reinforced composites are fabricated by weaving, knitting, knitting or stitching, and then reinforced in the thickness direction of the matrix material with the fiber fabric as reinforcement [6]. The composite structure is obtained by resin transfer moulding (RTM) or resin film infiltration (RFI) process. Three-dimensional fabric reinforced composites have high strength, high shear strength, high damage tolerance and strong ability to hinder crack growth. Moreover, they have been widely used in construction, national defense, aerospace and other fields because of their simple forming process and optimized structure design.

The purpose of this research is to theoretically analyze and predict the thermal conductivity of three-dimensional fabric reinforced composites. Using quartz fiber to weave three-dimensional fabric reinforced composites has the characteristics of high temperature resistance, corrosion resistance, thermal shock resistance and microwave transmission, which can meet the protection of warheads in a certain external environment [7-8]. The shape and structure of the fabric can be designed according to different requirements. Because of the simple preparation process, it is possible to develop three-dimensional fabric reinforced composites with excellent comprehensive properties under thermal and mechanical loads applied to missile flight. It is of great significance to develop and improve the application scope of three-dimensional fabric reinforced composites. This promotes the application of three-dimensional fabric reinforced composites in national defense construction, weapon manufacturing, aerospace and other fields. By studying the effects of different structural parameters, yarn reduction methods and weaving structures on thermal conductivity, the study of thermal conductivity of three-dimensional fabrics, the establishment of cell model and the exploration of thermal conductivity prediction methods have certain theoretical guiding significance [9]. This study provides a theoretical basis for the design of three-dimensional fabrics and the selection of parameters, and lays a foundation for the application of three-dimensional fabric reinforced composites in radome materials.

2. Measurement and Analysis of Heat Conductivity of Stereo Fabric Reinforced Composites

2.1. Measurement of thermal conductivity

The heat conduction performance test is carried out under constant temperature and humidity environment. The temperature and humidity are 20C and 65% RH. Because the material is anisotropic, it is necessary to cut the sample or adopt other pretreatment methods to ensure that the probe can coincide with the main direction of the sample, that is, the axial direction of the fiber reinforced material. (1) The thermal properties of the material can be measured by placing the probe between two flat surfaces of the sample. (2) Fix the sample/probe with fixture. (3) The whole test system should be placed in a sample chamber at constant temperature. (4) Balance the bridge before experiment. The initial resistance of the probe is between 1 and 50 ohms, and the current is guaranteed not to exceed 1mA by balancing the voltage of the bridge. (5) Apply thermal pulse to the sample and record the temperature within the pre-determined measuring time [10-14].

The temperature increase on the surface of the probe is recorded as a function of time. The temperature response in the sample is mainly related to the thermal diffusivity and thermal conductivity of the tested material. The thermal conductivity and thermal diffusivity of the tested material can be obtained by processing the recorded temperature curve. For isotropic materials, the temperature rise on the surface of the probe can be expressed as fear of lead.

$$\Delta T_s(\Theta) = \frac{P_0}{\pi^{3/2} r \lambda} H(\Theta) \quad (1)$$

Among them, p_0 is the input power; r is the radius of the probe; λ is the thermal conductivity of the sample material; $H(\Theta)$ is the dimensionless characteristic time function; H is the dimensionless time, which is defined as $\theta = \sqrt{Dt} / r$, where D is the thermal diffusivity of the sample and t is the measurement time. Thermal diffusion can be obtained by least square method to obtain the best linear relationship between ΔT_s and $H(\Theta)$. Finally, the thermal conductivity can be obtained from the slope of the straight line (1).

As for anisotropic materials, the temperature rise of the probe can be expressed as:

$$\Delta T_s(\Theta_T) = \frac{P_0}{\pi^{3/2} r (\lambda_L \lambda_T)^{-1}} H(\Theta_T) \quad (2)$$

λ_L and λ_T are the effective thermal conductivity of the samples in both longitudinal and transverse directions. Similar to the isotropic case, we first obtain the thermal diffusivity of D_T along the transverse direction of the sample. For a given volume specific heat ρc_p , we have:

$$\lambda_T = \rho c_p D_T \quad (3)$$

The longitudinal thermal conductivity λ_L of the sample can then be obtained from the slope of the line corresponding to equation (2).

Each parameter of quartz/epoxy composites consists of three samples, two of which are measured three times in turn, and three groups of measurement results are obtained. Finally, the average value of thermal conductivity of each sample is obtained.

The thermal conductivity of the composite pure epoxy resin is 0.1973w/(m · K) and that of the quartz fiber is 1.4w/(m · K) at ambient temperature of 20 C. The volumetric specific heat of three-dimensional braided composites with various parameters measured is shown in Table 1.

Table 1 Volume heat ratio of sample

Serial number	1#	2#	3#	4#	5#	6#	7#
Volume specific heat (MJ.m ⁻³ .K ⁻¹)	1.4142	1.3932	1.3637	1.393	1.4142	1.4098	1.3972
Serial number	8#	9#	10#	11#	12#	13#	14#
Volume specific heat (MJ.m ⁻³ .K ⁻¹)	1.4213	1.3883	1.4134	1.4193	1.4177	1.3695	1.3578
Serial number	15#	Three dimensional four directions		Three dimensional six directions		Lamination	2.5 D
Volume specific heat (MJ.m ⁻³ .K ⁻¹)	1.3873	1.4174		1.4122		1.3976	1.3918

The thermal conductivity of three-dimensional five-directional quartz/epoxy composites with different fiber volume fractions, different internal braiding angles and different yarn reduction methods was analyzed in the experiment (each of the three identical specimens is a group). The effects of braiding angle and volume fraction on the thermal conductivity of 3D 5d braided composites under different braiding parameters were obtained. The thermal conductivity of quartz/epoxy composites with the same volume fraction and different braiding structures was also analyzed, and the effects of various factors on the thermal conductivity of three-dimensional fabric reinforced composites were obtained.

2.2. Effect of braiding parameters on thermal conductivity of composites

Table 2 shows the average values of axial and radial thermal conductivity of three-dimensional five-directional quartz fiber/epoxy composites with different braiding parameters. The yarn fineness is 195texX2.

Table 2 Average thermal conductivity of three-dimensional five-directional composites

Number	Braided angle (°)	Volume fraction (%)	Axial thermal conductivity (W.m ⁻¹ .K ⁻¹)	Coefficient of variation(%)	Radial thermal conductivity (W.m ⁻¹ .K ⁻¹)	Coefficient of variation(%)
1#	19.9	46.5	0.4835	1.71	0.2748	1.34
2#	26.7	47.2	0.4574	2.82	0.2935	2.31
3#	31.8	45.9	0.4315	0.89	0.313	1.25
4#	21.8	51.4	0.5395	3.37	0.2999	2.61
5#	25.9	52.8	0.4761	2.65	0.3155	0.87
6#	32.7	49.3	0.4444	2.92	0.3581	1.67
7#	21.6	55.3	0.5534	1.99	0.3135	1.48
8#	25.5	57.1	0.5224	2.12	0.3377	2.24
9#	29.8	56.5	0.4938	1.27	0.3719	0.94
10#	21.8	61.7	0.5721	3.67	0.3368	1.74
11#	25.9	62.4	0.5448	2.73	0.3481	0.88
12#	31.8	60.7	0.5235	1.82	0.3841	1.93

2.2.1 Effect of axial heat conduction performance

With volume fraction as variable, its axial thermal conductivity is plotted as a broken line, as shown in Figure 1. Figure 1 is a broken line diagram of the axial thermal conductivity of three-dimensional quintuple quartz/epoxy composites with different fiber volume fractions under the same braiding structure and internal braiding angle.

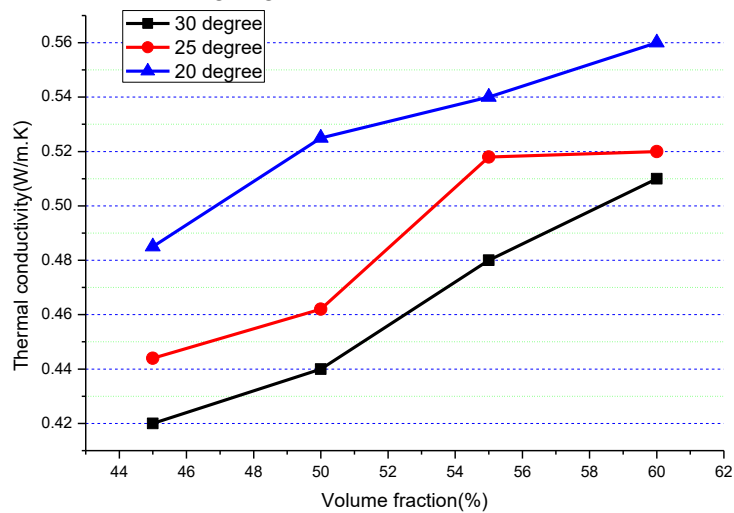


Figure 1 Axial thermal conductivity

It can be seen from Figure 1 that the axial thermal conductivity of the three-dimensional braided composites with 60% fiber volume fraction is 14.2% higher than that of the three-dimensional braided

composites with 45% fiber volume fraction when $\gamma = 20^\circ$ is equal to the internal braiding angle. When $\gamma = 25^\circ$ and $\gamma = 30^\circ$, the increase was 19.7% and 22.8% respectively. It shows that the axial thermal conductivity of three-dimensional braided composites increases with the increase of quartz fiber volume fraction. This is because the thermal conductivity of quartz fibers is higher than that of epoxy resin, so when the volume fraction of quartz fibers in the axial section increases, the heat transfer speed will be increased, which makes the thermal conductivity of three-dimensional braided composites larger.

2.2.2 The shadow of radial heat conductivity

The radial thermal conductivity is plotted as a polyline with volume fraction as a variable, as shown in Figure 2. Figure 2 shows the radial thermal conductivity of three-dimensional braided quartz/epoxy composites with different fiber volume fractions under the same braiding structure and internal braiding angle.

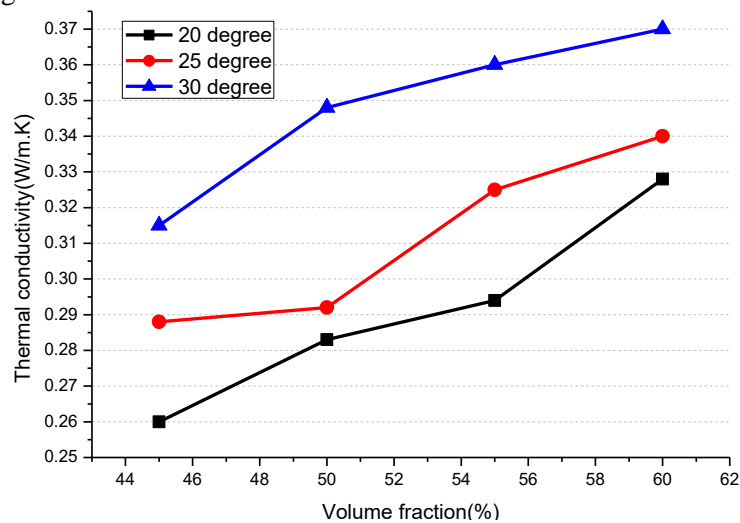


Figure 2 Radial thermal conductivity

It can be seen from Figure 2 that the radial thermal conductivity of the three-dimensional braided composites with 60% fiber volume fraction is 23.6% higher than that of the three-dimensional braided composites with 45% fiber volume fraction when $\gamma = 20^\circ$. When $\gamma = 25^\circ$ and $\gamma = 30^\circ$, they increased by 15.8% and 19.3% respectively. It shows that the radial thermal conductivity of three-dimensional braided composites increases with the increase of quartz fiber volume fraction. This is because the thermal conductivity of quartz fibers is higher than that of epoxy resin, so when the volume fraction of quartz fibers in the radial cross section increases, the heat transfer rate will be increased, which makes the thermal conductivity of three-dimensional braided composites larger.

As can be seen from Figure 1 and Figure 2, the internal braiding angle has opposite effects on the axial and radial heat conductivity of three-dimensional braided composites. The smaller the internal braiding angle of three-dimensional braided composites is, the more obvious the difference between the axial and radial thermal conductivity is. It can be seen that the thermal conductivity of three-dimensional braided composites shows significant anisotropy along the axial and radial directions, and the smaller the braiding angle is, the more obvious the anisotropy is.

3. Thermal Performance Prediction of Three-dimensional Fabric Reinforced Composites

3.1. Coefficient of thermal expansion

The thermal properties of materials refer to the different thermal and physical properties of materials and products in different temperature environments, including thermal expansion, thermal conductivity and thermal stability. Thermal expansion coefficient of materials can be divided into linear expansion coefficient and volume expansion coefficient. The use of linear expansion coefficient

is more common. It is defined as the relative change of the length of materials when the temperature rises 1 K. The linear expansion coefficient of three-dimensional fabric reinforced composites is studied in this paper.

$$\alpha = \frac{\Delta L}{L * \Delta T} \quad (4)$$

In the formula α is the linear expansion coefficient of the material, i.e. the relative change of the length of the sample when the temperature rises 1 K; L is the initial length of the sample; ΔT is the change of temperature; ΔL is the change of the length of the sample when the temperature changes. Because the coefficient of thermal expansion varies with temperature, the coefficient of thermal expansion obtained by formula (4) is the average value in the range of ΔL temperature.

3.2. Prediction of thermal expansion coefficient

In ABAQUS, heat transfer problems such as uncoupled heat transfer analysis, sequential coupled thermal stress analysis, fully coupled thermal stress analysis, adiabatic analysis and thermoelectric coupling analysis can be solved conveniently and quickly. The prediction of thermal expansion coefficient of materials requires sequential coupled thermal stress analysis using ABAQUS/Standard solver [15-18]. The results of stress-strain field depend on the results of temperature field. Therefore, the problem of temperature field, i.e. heat conduction, needs to be solved first, then the thermal stress analysis is carried out on the basis of known temperature field, and finally the stress-strain field can be obtained. In the process of analysis, the meshes used to solve the temperature field and stress-strain field can be the same or different. ABAQUS interpolates automatically.

The prediction of thermal expansion coefficient of composites is based on the finite element method to calculate the micro-mechanics. The method of measuring thermal expansion coefficient of composites by experiment is equivalent to the representative volume element of micro-scale. The sequential coupled thermal stress analysis of representative volume element is carried out in ABAQUS/Standard. The process of automatic prediction of thermal expansion coefficient of three-dimensional fabric reinforced composites by finite element software ABAQUS is as follows:

(1) Using Python language and ABAQUS secondary interface, the geometric model of representative volume elements of composite materials is automatically established and the meshes are reasonably divided.

(2) According to the research needs, the volume fraction of representative volume elements of composites is controlled at 50%.

(3) According to the orientation of matrix and reinforcement in composites, the orientation and properties of matrix and reinforcement are given respectively.

(4) Heat transfer analysis. Because the temperature of the sample increases slowly under the experimental conditions, it can be regarded as a steady-state heat transfer process in ABAQUS. In the thermal analysis mode, the initial temperature field is located at 20 degree C (room temperature) using a predefined field, and then the temperature of representative volume units is raised to the required temperature by applying temperature load. The temperature field distribution of representative volume units in the heating process is obtained.

(5) Thermal stress analysis. In the structural analysis mode, the temperature field distribution of representative volume elements is read into the thermal stress-strain analysis as a predefined field, and the corresponding boundary conditions are set.

(6) After the setting is completed, the calculation is submitted to obtain the micro-stress field distribution of the representative volume element of the composite material during the heating process. From the thermal stress distribution nephogram of representative volume units, it can be seen that the thermal stress caused by temperature field of fiber reinforced fabric is larger than that of epoxy resin matrix, which is due to the difference of elastic modulus and thermal expansion coefficient between epoxy resin and fiber. The displacement increment (ΔL) along the direction of predicting thermal expansion coefficient in the thermal stress-strain field of representative volume elements was extracted, and the thermal expansion coefficient of three-dimensional fabric reinforced composites was obtained by combining the formula (4). The calculated results are shown in Table 3 and compared with the experimental results as shown in Table 4 as well as Figure 3.

Table 3 Prediction results of thermal expansion coefficient of composite materials($10^{-6}/^{\circ}\text{C}$)

Structure layer	Temperature	X-direction thermal expansion coefficient	Y-direction thermal expansion coefficient	Z-direction thermal expansion coefficient
Structure layer one	Room temperature - 150 degrees	2.37	2.79	41.29
	Room temperature - 200 degrees	0.72	0.99	29.85
Structural layer two	Room temperature - 150 degrees	1.18	1.23	21.58
	Room temperature - 200 degrees	-0.22	-0.19	12.65
Structural layer three	Room temperature - 150 degrees	5.94	5.31	75.25
	Room temperature - 200 degrees	4.36	3.93	64.6
Structural layer four	Room temperature - 150 degrees	3.13	3.11	19.76
	Room temperature - 200 degrees	2.92	2.99	18.94

Table 4 Comparisons between predicted results and experimental results of thermal expansion coefficient of composites($10^{-6}/^{\circ}\text{C}$)(X direction)

Structure layer	Temperature	Prediction value of thermal expansion coefficient	Thermal expansion coefficient test value
Structure layer one	Room temperature - 150 degrees	2.37	2.37
	Room temperature - 200 degrees	0.72	0.73
Structural layer two	Room temperature - 150 degrees	1.18	1.12
	Room temperature - 200 degrees	-0.22	-0.23
Structural layer three	Room temperature - 150 degrees	5.84	5.93
	Room temperature - 200 degrees	4.36	4.11
Structural layer four	Room temperature - 150 degrees	3.13	2.82
	Room temperature - 200 degrees	2.92	2.97

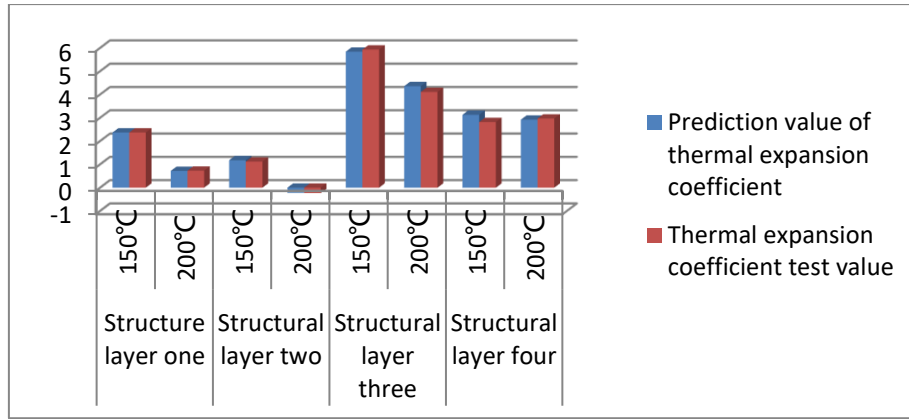


Figure 3 Contrast diagram of predicted value and experimented value

As can be seen from Table 4, the predicted results in this paper are basically consistent with the experimental results. The error range between the predicted values and the experimental values of the thermal expansion coefficient of three-dimensional fabric reinforced composites is within 5%. Moreover, the thermal expansion coefficients of three-dimensional fabric reinforced composites in X and Y directions are one order of magnitude smaller than those in Z directions. When aramid fiber fabric is used as reinforcement, the composites with negative thermal expansion coefficients can be designed[19-22].

4. Conclusion

In this paper, according to the performance requirements of reinforced composites, three-dimensional fabric reinforced composites are used as radome materials. According to the characteristics of variable cross section of reinforced composites, the effects of different yarn reduction methods and the distribution of yarn reduction points on the thermal conductivity of reinforced composites were studied. The thermal conductivity of samples with different knitting parameters and weaving structures was tested. The effects of different parameters, structures and yarn reduction methods on the thermal conductivity of three-dimensional fabric reinforced composites were analyzed. With the increase of internal braiding angle, the radial heat conductivity becomes stronger and the axial heat conductivity becomes weaker. The thermal conductivity of three-dimensional braided composites shows anisotropy along the axial and radial directions, and the smaller the braiding angle, the more obvious the anisotropy. In this paper, the effect of reinforcement on the properties of materials is studied. The thermal conductivity of three-dimensional fabric reinforced composites at room temperature is studied experimentally and theoretically. According to the use environment of materials, the thermal conductivity of three-dimensional fabric reinforced composites at high temperature can be studied when the test conditions permit. There are many kinds of three-dimensional fabrics. This paper mainly studies the three-dimensional five-dimensional structure. Although other structures have designed comparative experiments, there are fewer experimental pieces, which can only roughly compare their thermal conductivity. Some other parameters can also be added to the comparative experiments to evaluate the excellent thermal conductivity of different structures in more detail and accurately.

Acknowledgements

This work was supported by Natural Science Foundation of Hubei Province of China (Grant No.2018CFB681).

References

- [1] Hu Z, Karki R. Prediction of mechanical properties of three-dimensional fabric composites reinforced by transversely isotropic carbon fibers[J]. *Journal of Composite Materials*, 2015, 49(12),pp.1513-1524.

- [2] Babaeidarabad, Saman. Masonry Walls Strengthened with Fabric-Reinforced Cementitious Matrix Composite Subjected to In-Plane and Out-of-Plane Load[J]. *Journal of Composites for Construction*, 2013, 18(2), pp.68-70.
- [3] Laustsen S , Lund E , Kühlmeier, L, et al. Interfibre Failure Characterisation of Unidirectional and Triax Glass Fibre Non-Crimp Fabric Reinforced Epoxy Laminates[J]. *Applied Composite Materials*, 2015, 22(1), pp.51-79.
- [4] Jin L , Hu H , Sun B , et al. Three-point bending fatigue behavior of 3D angle-interlock woven composite[J]. *Journal of Composite Materials*, 2012, 46(8), pp.883-894.
- [5] Yan L . Sorption of humic acid to layered double hydroxides prepared through ion thermal method [J]. *DESALINATION AND WATER TREATMENT*, 2017, 93, pp.109-119.
- [6] Zhang Xiaotao, Wang Jiqiang, Wang Wei, et al. Elastic-plastic-creep response of multilayered systems under cyclic thermo-mechanical loadings [J]. *JOURNAL OF MECHANICAL SCIENCE AND TECHNOLOGY*, 2018,32(3), pp. 1227-1234.
- [7] Hong Meiling, Li Jie, Zhang Wenfeng, et al. Semimetallic 1T ' WTe₂ Nanorods as Anode Material for the Sodium Ion Battery [J]. *ENERGY & FUELS*, 2018, 32(5), pp. 6371-6377.
- [8] Zou Xuejun, Dong Yuying, Li Sijia, et al. Facile anion exchange to construct uniform AgX (X = Cl, Br, I)/Ag₂CrO₄ NR hybrids for efficient visible light driven photocatalytic activity [J]. *SOLAR ENERGY*, 2018, 169, pp.392-400.
- [9] Chen Shufang, Xu Zejun, Zhang Daohong, et al. Synthesis and application of epoxy-ended hyperbranched polymers [J]. *CHEMICAL ENGINEERING JOURNAL*, 2018,343,pp. 283-302.
- [10] Wen Zhipan, Ke Jun, Xu Jinlei, et al. One-step facile hydrothermal synthesis of flowerlike Ce/Fe bimetallic oxides for efficient As(V) and Cr(VI) remediation: Performance and mechanism [J]. *CHEMICAL ENGINEERING JOURNAL*, 2018, 343, pp.416-426.
- [11] Miao Ling, Zhu Dazhang, Liu Mingxian, et al. Cooking carbon with protic salt: Nitrogen and sulfur self-doped porous carbon nanosheets for supercapacitors [J]. *CHEMICAL ENGINEERING JOURNAL*, 2018, 347, pp.223-242.
- [12] Hong Hanyu, Shi Yu. Fast Deconvolution for Motion Blur Along the Blurring Paths [J]. *CANADIAN JOURNAL OF ELECTRICAL AND COMPUTER ENGINEERING-REVUE CANADIENNE DE GENIE ELECTRIQUE ET INFORMATIQUE*, 2018, 40(4), pp.226-274.
- [13] Zhang Xiaotao, Chen Haofeng, Ma Zhiyuan, et al. Shakedown boundaries of multilayered thermal barrier systems considering interface imperfections[J]. *INTERNATIONAL JOURNAL OF MECHANICAL SCIENCES*, 2018,144,pp.33-40
- [14] Gao Zhisheng, Xie Shenglong, Zhang bo, et al. Ultrathin Mg-Al layered double hydroxide prepared by ionothermal synthesis in a deep eutectic solvent for highly effective boron removal[J]. *CHEMICAL ENGINEERING JOURNAL*,2017,319,pp.108-118
- [15] **Chen Fengxi, Xie Shenglong, Huang XL, et al. Ionothermal synthesis of Fe₃O₄ magnetic nanoparticles as efficient heterogeneous Fenton-like catalysts for degradation of organic pollutants with H₂O₂ [J]. *JOURNAL OF HAZARDOUS MATERIALS*, 2017, 322(Si), pp.152-162**
- [16] **Xiang L, Li Z, Cheng J. Construction asphalt prepared by chemical treatment of deoiled asphalt [J]. *PETROLEUM SCIENCE AND TECHNOLOGY*, 2016, 34(10), pp.920-926**
- [17] Dong Shuhong, Zhou Jianqiu, Hui David. A quantitative understanding on the mechanical behaviors of carbon nanotube reinforced nano/ultrafine-grained composites [J]. *INTERNATIONAL JOURNAL OF MECHANICAL SCIENCES*, 2015, 101, pp.29-37
- [18] Wang Tielin, Jens KJ. Towards an understanding of the oxidative degradation pathways of AMP for post-combustion CO₂ capture [J]. *INTERNATIONAL JOURNAL OF GREENHOUSE GAS CONTROL*, 2015, 32, pp.354-361

- [19] Wang Guangxu, Zhou Jianqiu, Hu Shujuan, et al. Investigations of filling mass with the dependence of heat transfer during fast filling of hydrogen cylinders [J]. INTERNATIONAL JOURNAL OF HYDROGEN ENERGY, 2014, 39(9), pp.4380-4388
- [20] Liu XW, Chen LG, Wu F, et al. Optimal performance of a spin quantum Carnot heat engine with multi-irreversibilities [J]. JOURNAL OF THE ENERGY INSTITUTE, 2014, 87(1), pp.69-80
- [21] Huang Zhenghua, Zhang Yaozong, Li Qian, et al. Spatially adaptive denoising for X-ray cardiovascular angiogram images [J]. BIOMEDICAL SIGNAL PROCESSING AND CONTROL, 2018, 40, pp.131-139
- [22] Zhang Shuiping, Tian Xin, Xiong Chengyi, et al. Fast Implementation for the Singular Value and Eigenvalue Decomposition Based on FPGA [J]. CHINESE JOURNAL OF ELECTRONICS, 2017, 26(1), pp.132-136